Analysis of Electromagnetic Field Radiation from a Rectangular Cavity-Backed Slot Antenna Using ADI-FDTD Method

George M. Nyaory[1][*] Dominic B.O. K'Onditi[2] Heywood A. Ouma[3] Stephen Musyoki[1]

1. College of Engineering and Technology, School of Electrical, Electronic and Information Engineering, Jomo Kenyatta University of Agriculture and Technology, P.O.Box 62000-00200, Nairobi, Kenya
2. Faculty of Engineering, School of Electrical, Electronic and Information Engineering Multimedia University College of Kenya, P.O. Box 30305 - 00100. Nairobi, Kenya
3. School of Engineering, Department of Electrical and Information Engineering, University of Nairobi, P. O. Box 30197 – 00100, Nairobi, Kenya

 * E-mail of the corresponding author: gmnyaory@gmail.com

Abstract

In this paper, a rectangular Cavity Backed Slot Antenna (CBSA) Model excited by a probe is investigated. The analysis is carried out using the Alternating Direction Implicit - Finite Difference Time Domain (ADI-FDTD) Method which is applied to investigate its characteristics in terms of radiation patterns and power. This is because the method is capable of providing a more accurate definition of the electromagnetic fields within the rectangular apertures, while eliminating the Courant-Friedrich-Levy (CFL) stability condition which is present in the regular Finite Difference Time Domain (FDTD) method. A cavity-backed slot antenna structure with dimensions of 14cm×22cm×30cm is analyzed with the slot and aperture measurements done at 3GHz. Results showing current distribution on the material surrounding the apertures are presented and a discussion on the physical aspects of the aperture radiation phenomenon is also presented.

Keywords: cavity-backed slot antenna (CBSA), aperture radiation, alternating direction implicit-finite difference time domain (ADI-FDTD) method

1. Introduction

For a long time, slot cut on a conductor; both on a flat plate and on a curved surface have been investigated. The slot backed by the conducting flat plate such as parallel plate waveguide (Hirokawa, Ando & Goto 1992), rectangular waveguide (Stevenson 1948), rectangular cavity (Galejs 1963), radial line waveguide (Ando et al 1985) and many others (Elliot 1985) are very attractive since they belong to the flush-mounted structure that make them low profile. Research on the rectangular slotted-waveguide antenna has been extensively conducted because they are fundamental in modeling of array element of the very large aperture antennas such as planar slot array antenna (Ito 1988) and radial line slot antenna (Ando et al 1985) with a large number of elements.

The feeding structure of the CBSA is simple, free from conduction loss and dielectric loss, high power handling and is suitable for slot array applications. The field equations for the rectangular cavity backed slot antenna fed by a probe inside the cavity are established, with the infinite ground plane assumed outside the cavity. The Alternating Direction Implicit - Finite Difference Time-Domain (ADI-FDTD) Method is a vital tool in solving these equations (Zheng 1999) to obtain the electric and magnetic currents. The radiation patterns of the probe excited rectangular cavity backed slot antenna are investigated and presented in this paper.

2. Formulations

2.1 Model Analysis

The geometry of a rectangular waveguide is shown in Figure 1 from where a CBSA is derived. Solutions for TE modes are provided since they are excited at much lower operating frequencies than TM modes.
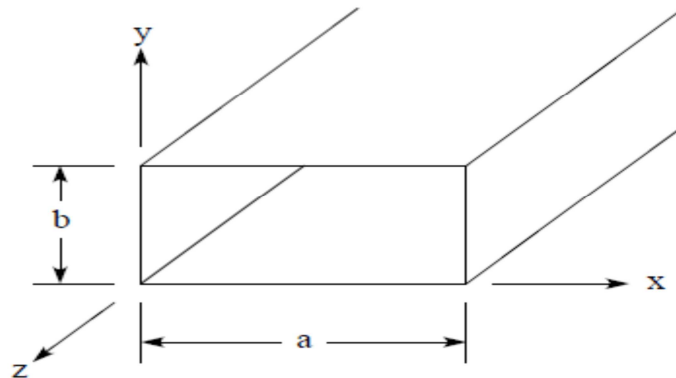

Figure 1. Geometry of rectangular waveguide

Figure 2 shows the geometry of the initial antenna design, which is similar to the one in (Li et al 2000). The antenna consists of a cavity of size 30cm × 22cm × 14cm fed by coaxial cable, connected to a slotted ground plane. The coaxial cable feed the cavity at the center of its wide face, at a distance of 7cm from the ground plane. All these parameters are depicted in Figure 2. This design is referred to as ''Original Design" in this paper.

To investigate the antenna characteristics, the following two assumptions are made;

- The cavity wall is made of perfect conductor and the thickness is negligible
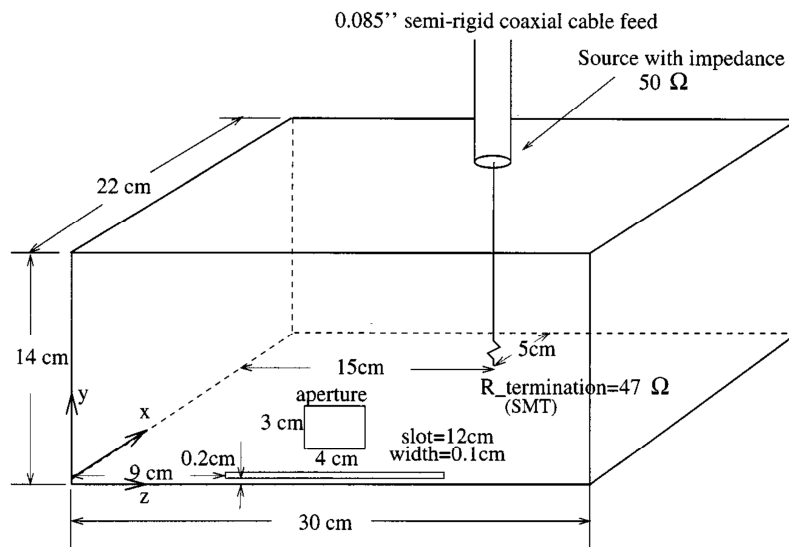- The probe is very thin in order to disregard its diameter.

Figure 2. A rectangular aperture antenna.

2.2. The relating equations

In order to gain insight into the radiating mechanism of the antenna, it is necessary to first understand the near-field quantities that are present on the structure. The cavity model aids in this pursuit since it provides a mathematical solution for the electric and magnetic fields of a slot antenna.

The approach to implementing the small aperture in the ADI-FDTD algorithm in this paper is based on the observation (Omiya et al 1998; Hikage et al 2001) that all electrically small apertures can be modeled by equivalent induced electric and magnetic dipoles if the fields are observed sufficiently far from the aperture.

Balanis (1982) uses the vector potential approach to find the following solution for the E- field and H-field distributions of the TE$_{mn}$ modes as represented in the following equations:

E – Field

$$E_x = A_{mn} \frac{k_y}{\varepsilon} \cos(k_x x) \sin(k_y y) e^{-jk_z z} \tag{1}$$

$$E_y = -A_{mn} \frac{k_x}{\varepsilon} \sin(k_x x) \cos(k_y y) e^{-jk_z z} \tag{2}$$

$$E_z = 0 \tag{3}$$

H - Field

$$H_x = A_{mn} \frac{k_x k_z}{\omega \mu \varepsilon} \sin(k_x x) \cos(k_y y) e^{-jk_z z} \tag{4}$$

$$H_y = A_{mn} \frac{k_y k_z}{\omega \mu \varepsilon} \cos(k_x x) \sin(k_y y) e^{-jk_z z} \tag{5}$$

$$H_z = -jA_{mn} \frac{k_c^2}{\omega \mu \varepsilon} \cos(k_x x) \cos(k_y y) e^{-jk_z z} \tag{6}$$

Where, $k_x = \frac{m\pi}{a} = \frac{2\pi}{\lambda_x}$, $m = 0,1,2,...$; $k_y = \frac{n\pi}{b} = \frac{2\pi}{\lambda_y}$, $n = 0,1,2,...$; for $m = n \neq 0$ and m, n are integers; $k_z = \beta \sqrt{1 - \left(\frac{\lambda}{\lambda_c}\right)^2} = \beta \sqrt{1 - \left(\frac{f_c}{f}\right)^2}$, and A_{mn} is the amplitude coefficient.

In the above equations, f and f_c represent the operating frequency and cut-off frequency, respectively.

$$(f_c)_{mn} = \frac{1}{2\pi\sqrt{\mu\varepsilon}} \sqrt{\left(\frac{m\pi}{a}\right)^2 + \left(\frac{n\pi}{b}\right)^2} \qquad m, n = 0,1,2,... \tag{7}$$

$$(k_c)_{mn} = \sqrt{k_x^2 + k_y^2} = \frac{2\pi}{\lambda_c} \tag{8}$$

Equations (1-3) and (5-6) give the field distributions of the propagating modes. The equivalent electric and magnetic current densities may be obtained using:

$$\vec{J} = \hat{n} \times \vec{H} \tag{9}$$

$$\vec{M} = -\hat{n} \times \vec{E} \tag{10}$$

Where $\hat{n}$ is the outward directed surface normal. The magnetic field is zero along the x=0 and x=a walls and is normal to the surface along the y=0 and y=b walls. Therefore, no equivalent electric current density flows on the walls of the cavity. The electric field results in a non-zero magnetic current density on the walls of the cavity.

2.3. ADI-FDTD Scheme

The FDTD method from where ADI-FDTD is derived uses a discretization in time and space to calculate a solution of Maxwell's curl equations directly in the time domain (Mittra & Lee 1971):

$$\nabla \times \vec{E} = -\mu \frac{\partial \vec{H}}{\partial t} \tag{11}$$

$$\nabla \times \vec{H} = -\varepsilon \frac{\partial \vec{E}}{\partial t} + \vec{J} \tag{12}$$

Rearranging these equations, with $\vec{J} = \sigma \vec{E}$, we obtain

$$\frac{\partial \vec{H}}{\partial t} = -\frac{1}{\mu} \nabla \times \vec{E} \tag{13}$$

$$\frac{\partial \vec{E}}{\partial t} = -\frac{1}{\varepsilon} \nabla \times \vec{H} - \frac{\sigma}{\varepsilon} \vec{E} \tag{14}$$

Evaluating the vector curl operator $(\nabla \times \vec{A})$ and employing central differencing in both time and space to approximate the partial derivatives, we obtain six update equations (one for each component of the electric and magnetic fields). For example, the update equation for the E_x component is as follows:

$$E_x^n(i,j,k) = \left[\frac{\varepsilon}{\varepsilon + \sigma \Delta t}\right] E_x^{n-1}(i,j,k) + \left[\frac{\Delta t}{\varepsilon + \sigma \Delta t}\right] \left[\frac{H_z^{n-1/2}(i,j,k) - H_z^{n-1/2}(i,j-1,k)}{\Delta y} - \frac{H_y^{n-1/2}(i,j,k) - H_y^{n-1/2}(i,j,k-1)}{\Delta z}\right] \tag{15}$$

The electromagnetic structure is modeled by approximating its geometry and composition with Yee cells (Taflove & Hagness 2000; Taflove 1998) of different material parameters; both conductivity and relative dielectric constant.

In an isotropic medium with the medium permittivity ε and the medium permeability μ, the curl vector equation of Maxwell's equations can be cast into six scalar partial differential equations in the Cartesian coordinates. For simplicity, the corresponding central difference form in ADI-FDTD (Taflove 1998) is;

Step 1

$$\begin{bmatrix} \varepsilon_{i+\frac{1}{2},j,k} \dfrac{E_x\big|_{i+\frac{1}{2},j,k}^{n+\frac{1}{2}} - E_x\big|_{i+\frac{1}{2},j,k}^{n}}{\frac{\Delta t}{2}} \\[2ex] +\sigma_{i+\frac{1}{2},j,k} \dfrac{E_x\big|_{i+\frac{1}{2},j,k}^{n+1/2} - E_x\big|_{i+\frac{1}{2},j,k}^{n}}{2} \end{bmatrix} = \begin{bmatrix} \dfrac{H_z\big|_{i+\frac{1}{2},j+1/2,k}^{n+\frac{1}{2}} - H_z\big|_{i+\frac{1}{2},j-1/2,k}^{n+1/2}}{\Delta y} \\[2ex] -\dfrac{H_y\big|_{i+\frac{1}{2},j,k+1/2}^{n} - H_y\big|_{i+\frac{1}{2},j,k-1/2}^{n}}{\Delta z} \end{bmatrix} \tag{16}$$

Step 2

$$\begin{bmatrix} \varepsilon_{i+\frac{1}{2},j,k} \dfrac{E_x\big|_{i+\frac{1}{2},j,k}^{n+1} - E_x\big|_{i+\frac{1}{2},j,k}^{n+1/2}}{\frac{\Delta t}{2}} \\[2ex] +\sigma_{i+\frac{1}{2},j,k} \dfrac{E_x\big|_{i+\frac{1}{2},j,k}^{n+1} + E_x\big|_{i+\frac{1}{2},j,k}^{n+1/2}}{2} \end{bmatrix} = \begin{bmatrix} \dfrac{H_z\big|_{i+\frac{1}{2},j+1/2,k}^{n+\frac{1}{2}} - H_z\big|_{i+\frac{1}{2},j-1/2,k}^{n+1/2}}{\Delta y} \\[2ex] -\dfrac{H_y\big|_{i+\frac{1}{2},j,k+1/2}^{n+1} - H_y\big|_{i+\frac{1}{2},j,k-1/2}^{n+1}}{\Delta z} \end{bmatrix} \tag{17}$$

2.4. Computational Model

In order to simulate an antenna using ADI-FDTD the geometry is first modeled in the computational space (Maloney & Smith 1993; Li et al 1999; Taflove 1998). This is a tedious process since care needs to be taken so that all of the important details of the antenna are modeled properly. In many cases this is an iterative process that involves correcting errors and determining how finely certain details need to be modeled.

The ADI-FDTD and FDTD methods have been merged and implemented within the same solver using SEMCAD-X software. Both methods share the same spatial discretization and modeling features, thus excluding from the comparison the influence of factors external to the time integration schemes.

The computational domain is truncated by the uniaxial perfectly matched layer (UPML) (Taflove & Hagness 2000) and absorbing boundary condition (ABC) modified in order to retain the unconditional stability of ADI-FDTD. Typical modeling features such as plane wave excitations, voltage sources and R,L,C lumped elements have also been included (Maloney & Smith 1993).

An excitation is then applied to the computational model and the $\vec{E}$ field and $\vec{H}$ field computations are alternately matched through time from time zero to the desired stopping point. Results can be viewed either

in the time domain or in the frequency domain. In order to obtain the frequency characteristics of the antenna it is necessary to compute a fast-Fourier transform (FFT) of the transient output data.

The techniques presented above allow antennas to be modeled in fine detail (Lei et al 2007). Feed lines, finite ground planes, and case enclosures can all be included in the computational model. In addition, the techniques are highly generalized so a number of different antennas can be analyzed.

The unknown magnetic current sheet along the slot and electric current on the probe can be determined by applying ADI-FDTD. The excitation of the antenna was selected for dominant mode operation at a center frequency of f_c = 3 GHz which is within the wifi frequency of operation.

3. Results

3.1 Current Distribution

Figures 3 show the field's equivalent current densities of the radiating slots as present in the cavity model.

(a) ADI-FDTD simulated E-field
distribution in back plane

(b) ADI-FDTD simulated E-field
distribution in front plane
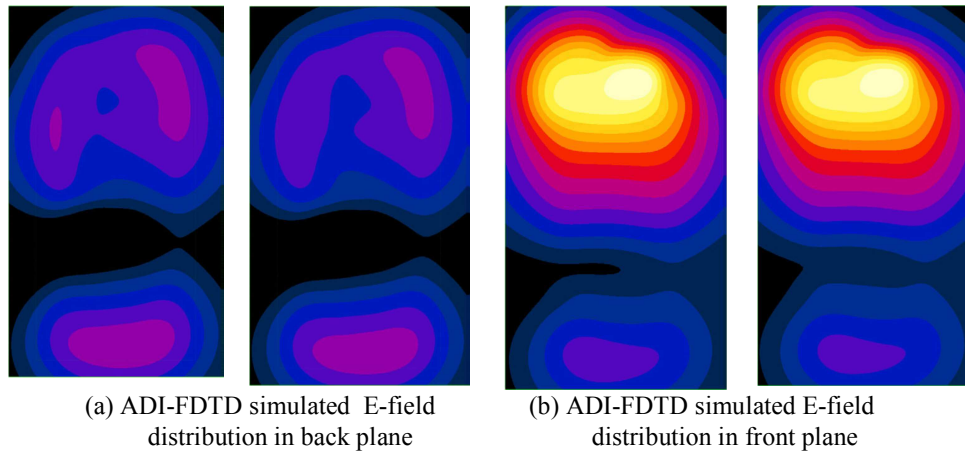
Figure 3. A rectangular aperture field distributions

3.2. Power distribution

The relationship of energy conservation in the ADI-FDTD simulation for the antenna radiation problem is presented. Considering a short dipole (see the inset in Figure 2), which is simulated by the Software. We assume that the dipole arms are PEC. A voltage excitation is used to excite the dipole during simulation of the radiation power. Integrating the Poynting vector on the surface of the enclosed box, the input power should equal to the radiation power for a lossless system, namely, satisfy the following relationship:

$$\frac{1}{2}Re\left(\iiint_v \vec{E} \cdot \vec{J}^* \, \partial v\right) = \frac{1}{2}Re\left(\oiint_s \vec{E} \cdot \vec{H}^* \partial \vec{s}\right) \tag{18}$$

Where, V is the source region and S is the surface of Huygens' box, respectively. Since we add the excitation to the electric field, the relationship between the E and J can be expressed as:

$$E^{n+1}(i,j,k) = \frac{\Delta t}{\varepsilon + 0.5\sigma\Delta t} J^{n+\frac{1}{2}}(i,j,k) \tag{19}$$

The conductivity of the dipole element is calculated using the formula:

$$\sigma = \frac{LR}{D} \tag{20}$$

Where, R, L and D are the resistance, length and size of cross section of the dipole, respectively.

For a lossy system, the input power should equal to the radiation plus the dissipated power.

$$\frac{1}{2} Re\left(\iiint_v \vec{E} \cdot \vec{J}^* \, \partial v\right) = \frac{1}{2} Re\left(\oiint_s \vec{E} \cdot \vec{H}^* \partial \vec{s}\right) + \frac{1}{2} \sigma |E|^2 \qquad (21)$$

Where the electric field, E, inside the integral of the left hand side is measured at the excitation point; the electric and magnetic fields, E and H, in the first term of the right hand side are measured on the closed surface; and the electric field E in the second term of the right hand side is measured inside the lumped element. The incident, radiated and dissipated power value are plotted in Figure 4.
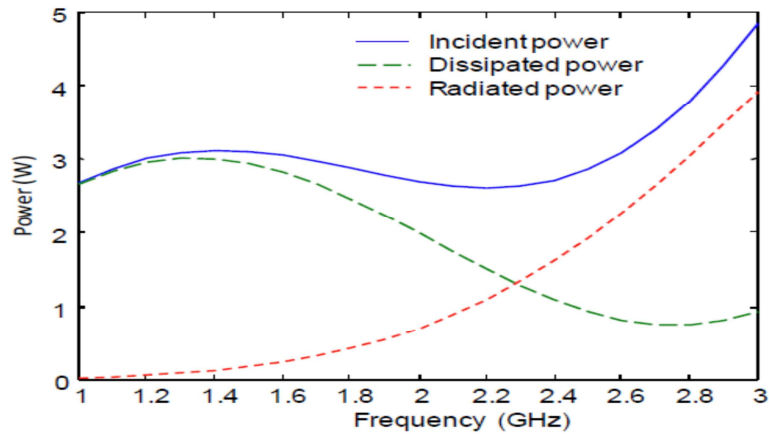
Figure 4. Radiated, dissipated and incident power simulated by using ADI-FDTD code.

3.3. Radiation pattern

To validate the results, the design presented in (Tan, W., Z. Shen, and Z. Shao 2008) is modeled with SEMCAD X. Once the far zone fields are known, the radiation pattern can be presented as in Figure 5 and 6 for the original design and for ADI-FDTD model respectively. The configuration is designed and optimized to suppress side radiation from an infinitesimal dipole, which has an omnidirectional radiation pattern within the cavity. This focuses the radiation in the direction of the main lobe while improving the gain, with a minimum effect on the antenna return loss level and impedance bandwidth.

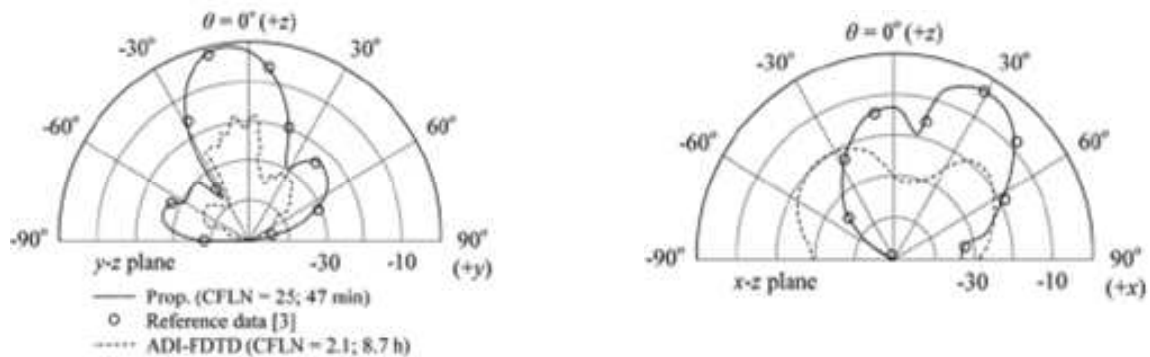Figure 5. Radiation patterns of the original design (Tan, W., Z. Shen, and Z. Shao 2008)
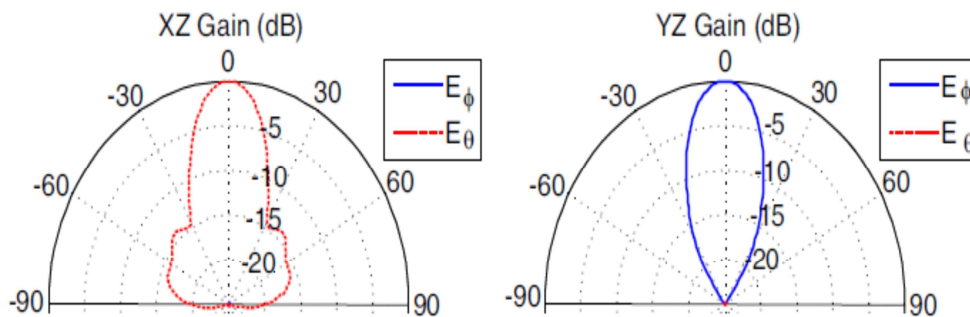
Figure 6. Radiation patterns as computed using software

4. Conclusion

The radiation pattern of probe excited rectangular cavity-backed slot antenna for high gain applications obtained using the ADI-FDTD method is presented in this paper. The differential field equations for the infinite ground plane assumed outside the cavity are first established for the unknown current over the slot and along the probe. These currents can be solved by ADI-FDTD Method.

Both ADI-FDTD and FDTD simulations show that the energy is mostly radiated out of the front of the cavity through the high E-fields located above the antenna. This is desirable because the energy is thus directed away from the radiator, as intended with the use of an integrated antenna.

The method can be readily extended to evaluate the enclosures with other geometries. It also can be applied to a variety of problems that involve coupling between metallic enclosures through an aperture.

References

Ando, M., et al. (1985), "A radial line slot antenna for 12 GHz satellite TV reception." *IEEE Trans. Antennas Propag.* **33**(12), 1347-1353

Balanis, C., "Antenna Theory". (1982), *2nd Ed., John Wiley & Sons, New York*

Elliott, R.S. (1985), "Antenna Theory and Design" *India: Prentice hall*, 86-91.

Galejs, J. (1963), "Admittance of rectangular slot which is backed by a rectangular cavity" *IEEE Trans. Antennas Propag.* **11**(3), 119-126

Hikage, T., Omiya, M., and Itoh, K., (2001), "Considerations on performance evaluation of cavity-backed slot antenna using the FDTD technique," *IEEE Trans. Antennas Propag.,* **49**(12), 1712–1717

Hirokawa, Ando, J.M and Goto, (1992), "Waveguide-fed parallel plate slot array antenna" *IEEE Trans. Antennas Propag.* **40**, 2218-223

Ito, K. (1988), "Planar antenna for satellite reception." *IEEE Trans. Broadcasting*. **34**(4), 457-464.

Lei, J.Z., Liang, C.H., and Zhang Y. (2007), " Study On Shielding Effectiveness of Metallic Cavities With Apertures By Combining Parallel FDTD Method With Windowing Technique" *Progress In Electromagnetics Research, PIER* **74***, 85–112*

Li, M., Drewniak, J. L., Hubing, T.H., VanDoren, T. P., (1999), "Slot and aperture coupling for air flow aperture arrays in shielding enclosure designs", *IEEE Electromagnetic Compatibility Symposium Proceedings, Seattle,* WA

Li, M., Nuebel, J., et al. (2000) "EMI from Cavity Modes of Shielding Enclosures—FDTD Modeling and Measurements" *IEEE Transactions on Electromagnetic Compatibility,* **42**(1)

Maloney, J.G. and Smith, G.S. (1993), "A Comparison of methods for modeling electrically thin dielectric and conducting sheets in the finite-difference time-domain method." *IEEE Trans. Antennas Propag.,***41**(5), 690-694

Mittra R. and Lee S.W. (1971), "Analytical Techniques in the Theory of Guided Waves*," The Macmillan Company; New York*

Omiya, M., Hikage, T., Ohno, N., Horiguchi, K., and Itoh, K., (1998), "Design of cavity-backed slot antennas using the finite-difference time-domain technique," *IEEE Trans. Antennas Propag.,***46**(12), 1853–1858

Stevenson, A.F, (1948), "Theory of slots in rectangular wave-guides*." J. Appl. Phy*. **19**(1), 24-38.

Taflove A., (1998), "Advances in Computational Electrodynamics: The Finite-Difference Time-Domain Method." *Artech House, Boston*

Taflove, A., and Hagness, S. (2000), "Computational Electrodynamics: The Finite-Difference Time-Domain Method, "*2 ed., Artech House, Boston, MA*

Zheng, F. (1999), "Novel Unconditionally Stable Finite-Difference Time-Domain Method for Electromagnetic and Microwave Modeling" *Submitted in partial fulfillment of the requirements for the Degree of Doctor of Philosophy; major subject: Electrical and Computer Engineering,* Dalhousie University.

Tan, W., Z. Shen, and Z. Shao, (2008) "Radiation of high-gain cavity-backed slot antennas through a two-layer superstrate," *IEEE Antennas and Propagation Magazine*, **50**(3), 78-87.